

Phase Difference of Electron Cyclotron Harmonic (ECH) Waves Observed by Using the Interferometry Observation Mode of the Arase Satellite

Tomoe Taki, Satoshi Kurita, Airi Shinjo, Satoko Nakamura, Hirotsugu Kojima, Yoshiya Kasahara, Shoya Matsuda, Ayako Matsuoka, Yoshizumi Miyoshi, and Iku Shinohara

Abstract – We report on the observation of phase differences of electron cyclotron harmonic (ECH) waves by attempting interferometric observations performed by the Arase satellite. The electric field spectra of ECH waves observed by the Arase satellite show a case that multiple peaks in intensity exist between integer multiples of the electron cyclotron frequency. Calculation of the phase difference at the frequencies of these peaks indicated that the phase differences were different even at close frequencies. Even though the phase differences obtained from the observations potentially have an ambiguity of $2n\pi$, it is difficult to argue that the phase velocity significantly changes at close frequencies. It is, thereby, possible that the wave vector directions of the ECH waves are different at the frequencies of the intensity peaks.

Manuscript received 28 December 2022. The funding information is Grant Numbers JPMJSP2110, 20H01959, 21H01146, 21H04520, 21K13978, and 22K03699.

Tomoe Taki and Airi Shinjo are with the Graduate School of Engineering, Kyoto University, Gokasho, Uji City, Kyoto Prefecture 6110011, Japan; e-mail: taki.tomoe.75n@st.kyoto-u.ac.jp, airi_shinjo@rish.kyoto-u.ac.jp.

Satoshi Kurita and Hirotsugu Kojima are with the Research Institute for Sustainable Humanosphere, Kyoto University, Gokasho, Uji City, Kyoto Prefecture 6110011, Japan; e-mail: kurita.satoshi.8x@kyoto-u.ac.jp, kojima.hirotsugu.6m@kyoto-u.ac.jp.

Satoko Nakamura is with Institute for Advanced Research, Nagoya University, Furo-cho, Chikusa-ku, Nagoya City, Aichi Prefecture 4648601, Japan; e-mail: nakamura.satoko@isee.nagoya-u.ac.jp.

Yoshiya Kasahara and Shoya Matsuda are with the Graduate School of Natural Science and Technology, Kanazawa University, Kakuma, Kanazawa City, 9201192, Japan; e-mail: kasahara@staff.kanazawa-u.ac.jp, matsuda@staff.kanazawa-u.ac.jp.

Ayako Matsuoka is with Data Analysis Center for Geomagnetism and Space Magnetism Graduate School of Science, Kyoto University, Kitashirakawa-Oiwake Cho, Sakyo-ku Kyoto 606-8502, Japan; e-mail: matsuoka@kugi.kyoto-u.ac.jp.

Yoshizumi Miyoshi is with Institute for Space-Earth Environmental Research, Nagoya University, Furo-cho, Chikusa-ku, Nagoya City, Aichi Prefecture 4648601, Japan; e-mail: miyoshi@isee.nagoya-u.ac.jp.

Iku Shinohara is with Institute of Space and Astronautical Science, Japan Aerospace Exploration Agency, 3-1-1 Yoshinodai, Chuo-ku, Sagami-hara City, Kanagawa Prefecture, 252-5210, Japan; e-mail: iku@stp.isas.jaxa.jp.

1. Introduction

Electron cyclotron harmonic (ECH) waves are one of the plasma waves observed in the magnetosphere. These waves are characterized by a harmonic structure with peaks between integer multiples of the electron cyclotron frequency f_{ce} . ECH waves are electrostatic. The wave vector is approximately perpendicular to the background magnetic field, and the electric field oscillations are parallel to the wave vector. An ECH wave was first observed by the Orbiting Geophysical Observatory-5 satellite [1] and was observed in the magnetosphere of the Earth and other planets and satellites [2–5]. An ECH wave was reported to have large amplitudes [1, 6], suggesting that it affects the plasma environment and was shown to cause pitch angle scattering [7, 8], which generates diffuse auroras [9]. Because the dispersion relation of ECH waves strongly depends on the parameters of cold electrons, it is possible to estimate the plasma environment, such as the background electron temperature, from the phase velocity of ECH waves.

In this study, we report on the observation of ECH waves using the interferometry observation mode of the Arase satellite. We analyzed the phase difference of the ECH wave observed by using the interferometry technique. It was suggested that the ECH wave has multiple peaks in each frequency band and that the wave vector may be different in each frequency.

2. Phase Difference of ECH Waves Observed by Interferometry Observation of the Arase Satellite

2.1 Instruments and Method

This study used electric field wave data observed by the Plasma Wave Experiment (PWE) on the Arase satellite. The Magnetic Field Experiment (MGF) was also used to determine the direction of the ambient magnetic field. The Arase satellite observed the Earth's magnetosphere and was located in an elliptical orbit of 300 km at perigee and 5.1 Re (Earth radius: 6371 km) at apogee [10]. The satellite was spin stabilized with a spin period of 8 s. The spin axis was roughly directed toward the Sun. The PWE had two pairs of wire probe antennas (WPT) on the spin plane [11] and a three-axis magnetic search coil (MSC). Signals obtained by the WPT and MSC were received by the Onboard Frequency

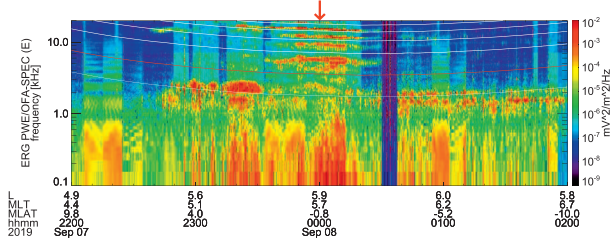


Figure 1. Overview of the electric field spectrum observed by OFA from 22:00 UT on September 7, 2019, to 2:00 UT on September 8, 2019.

Analyzer (OFA) and waveform capture (WFC) in the frequency range of a few hertz to 20 kHz. The normal sampling frequency of WFC is 65,536 Hz. Because waveform data obtained by WFC had a large data size, waveforms were intermittently obtained. The OFA provided instantaneous frequency spectrum data every second [12]. The MGF measured the ambient magnetic field vectors [13]. It was used to compare wave data to determine the direction of oscillation of the electric field of the wave and also to calculate the electron cyclotron frequency because it provided the magnitude of the background magnetic field at the satellite location.

The four antennas of the WPT are 15.6 m long and named $U1$, $U2$, $V1$, and $V2$, respectively. Normally, the electric field waveforms Eu and Ev were observed by using the pair of antennas ($U1-U2$, and $V1-V2$) as dipole antennas. There was also an observation mode in which only $V1$ and $V2$ were used as monopole antennas. In this mode, the potential difference between each antenna and the spacecraft body was observed. It was equivalent to an interferometry observation between antennas $V1$ and $V2$.

The electric field waveforms observed at antennas $V1$ and $V2$ were called $Ev1$ and $Ev2$, respectively. Due to the phase velocity of ECH waves, a phase difference of observed ECH waves was expected between $Ev1$ and $Ev2$. The following shows the calculation method of the phase difference:

$$W_i(f) = \mathcal{F}[E_{Vi}(f)] \quad (i = 1, 2) \quad (1)$$

$$\theta_i(f) = \arctan(W_i(f)) \quad (2)$$

$$\Delta\theta(f) = \theta_1 - \theta_2 \quad (3)$$

where W_1 and W_2 are the complex Fourier transforms of antennas $Ev1$ and $Ev2$.

2.2 Event Analysis

The analysis was performed for the ECH waves observed near 00:00 Universal Time (UT) on September 8, 2019. An overview of the electric field spectra observed by OFA is shown in Figure 1. The electron cyclotron frequency f_{ce} calculated using the MGF background field data is indicated by the red line in the figure, and its half and integer multiples are

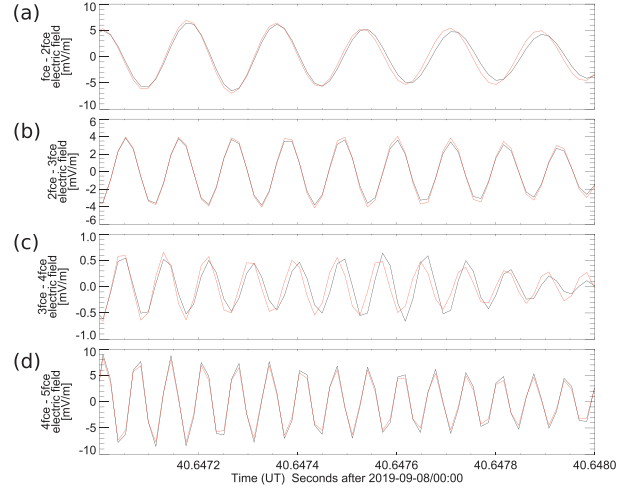


Figure 2. Electric field waveforms observed from 00:00:40.647 UT for 1 ms, which are bandpass filtered in the frequency of (a) f_{ce} to $2f_{ce}$, (b) $2f_{ce}$ to $3f_{ce}$, (c) $3f_{ce}$ to $4f_{ce}$, and (d) $4f_{ce}$ to $5f_{ce}$, respectively.

indicated by the white lines. There was a harmonic structure with peaks between integer multiples in the frequency range above f_{ce} . The burst mode operation of interferometric observations was continuously performed for 60 s, starting at 00:00:10 UT. The time of operation of interferometry observation is arrowed in Figure 1. The magnetic local time (MLT) at this time is 5.7 MLT, the radial distance is 5.9 R_e , and the magnetic latitude is -0.8° . Figure 1 shows that there are multiple peaks in the electric field spectrum in the frequency band between f_{ce} and $2f_{ce}$, especially around 00:00 UT on September 8, 2019.

The waveforms from 00:00:40.647 UT during 1 ms are shown in Figure 2. At this time, the elevation angle from the spin plane in the direction of the background magnetic field was 4° , and the angle that the background magnetic field projected onto the spin plane made with the antenna $Ev1$ was -85° . At this time, the electric field waveforms with an amplitude of about 40 mV/m were seen in both $Ev1$ and $Ev2$. The wave vector direction, which coincides with the direction of oscillation of the electric field, is considered to have a component parallel to the antenna. Figure 2 shows bandpass-filtered electric field waveforms in the harmonic bands of the ECH wave. The black and red line in each figure shows the bandpass-filtered $Ev1$ and $Ev2$ waveform, respectively. The two lines did not overlap, and a phase difference was obtained. The phase difference was calculated by Fourier transform using 1024 points so that the peaks of these frequencies were visible. The frequency resolution was 64 Hz. The Hanning window was used to perform the Fourier transform, which is expressed as

$$w(k) = \alpha - (1 - \alpha) \cos\left(\frac{2\pi k}{N}\right) \quad (0 \leq k \leq N - 1) \quad (4)$$

We used $\alpha = 0.5$. The time used was approximately 15.6 ms centered at 00:00:40.647 UT. The frequency and

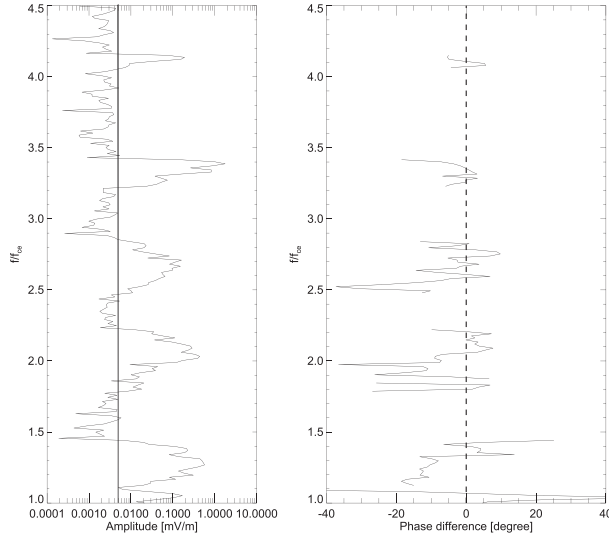


Figure 3. (Left) Amplitude and (right) phase difference between Ev1 and Ev2 derived from the PWE/WFC observation at 00:00:40.647 UT on September 8, 2019, as a function of normalized frequency by f_{ce} . The vertical line in the left figure indicates the threshold value of 0.005 mV/m.

amplitude and frequency and phase difference are shown in Figure 3. The vertical axis was normalized by f_{ce} . The phase difference at each frequency was calculated if the wave amplitude in the band exceeded 0.005 mV/m to remove the fluctuations of the phase difference caused by the low intensity waves and noises. From the left panel of Figure 3, we see that the intensity peaks in the harmonic bands of the ECH waves are greater than 0.1 mV/m. Among the intensity peaks, low intensity waves or noises are present with the intensity below 0.005 mV/m. Thus, we selected the threshold value of 0.005 mV/m to discriminate the ECH waves and noises. Figure 3 shows that multiple peaks are included between integer multiples of the cyclotron frequency. The multiple peaks at f_{ce} to $2f_{ce}$ were remarkable, but the other frequency bands also contain multiple peaks with gaps rather than a single peak.

3. Discussion and Conclusion

Figure 3 shows that the signs of the phase difference may be different even though the frequencies are close. For example, at 4672 Hz ($1.052 f_{ce}$), the phase difference was 20.08° , and at 5312 Hz ($1.196 f_{ce}$), the phase difference was -13.01° . Because these phase differences are expressed in the range of -180° to 180° , the actual phase differences are shown as follows:

$$\Delta\theta = \Delta\theta_{\text{observed}} + 2n\pi \quad (5)$$

where n is an integer, $\Delta\theta$ is the true phase difference between the two observation points, and $\Delta\theta_{\text{observed}}$ is the phase difference calculated from the observed waveform. There are other frequency bands with positive and negative phase differences at close frequencies. At 15,040 Hz ($3.39 f_{ce}$), the phase difference is -3.58° , and

Ev1 is later than Ev2, while at 14,848 Hz ($3.34 f_{ce}$), the phase difference is 0.270° , and Ev1 is earlier than Ev2. As shown in (4), the true phase difference has ambiguity, but it is difficult to argue that the phase velocity significantly differs at close frequencies, considering that they follow the same dispersion curve. Therefore, this difference in phase difference may be due to a difference in the direction of the wave vector. In this case, it is suggested that the wave vector may be different for each frequency. There may be multiple small-scale source regions distributed around the Arase satellite. Another cause may be the mixing of multiple ECH waves with different peak frequencies. In the harmonic structure shown in Figure 1, the fundamental appears to have a single peak in the early part of the event before 00:00 UT on September 8, 2019, and peaks in multiple frequency bands with gaps in between in the latter half of the event. It is quite difficult to determine from the spectral changes whether the ECH waves seen in this event are a single wave or a mixture of multiple ECH waves.

We reported on the observation of phase differences in the ECH waves by attempting interferometric observations for the ECH waves. The electric field spectra of ECH waves observed between 22:00 UT on September 7, 2019, and 2:00 UT on September 8, 2019, showed the existence of multiple peaks of intensity between integer multiples of the cyclotron frequency. Calculation of the phase difference for each of these peaks indicated that the phase differences were different even at close frequencies. Even though the phase differences obtained from the observations have an ambiguity of $2n\pi$, it is difficult to argue that the phase velocity changed that much at close frequencies. It is, thereby, possible that the wave vector direction was different at each frequency.

4. Acknowledgments

Scientific data of the Arase (formerly known as Exploration of energization and Radiation in Geospace [ERG]) satellite were obtained from the ERG Science Center operated by the Institute of Space and Astronautical Science, Japan Aerospace Exploration Agency, and the Institute for Space-Earth Environmental Research, Nagoya University (<https://ergsc.isee.nagoya-u.ac.jp/index.shtml.en>).

5. References

1. C. Kennel, F. Scarf, R. Fredricks, J. McGehee, and F. Coroniti, "VLF Electric Field Observations in the Magnetosphere," *Journal of Geophysical Research*, **75**, 31, November 1970, pp. 6136-6152.
2. H. Oya, "Plasma Flow Hypothesis in the Magnetosphere Relating to Frequency Shift of Electrostatic Plasma Waves," *Journal of Geophysical Research*, **80**, 19, July 1975, pp. 2783-2789.
3. A. Shinbori, T. Ono, M. Iizima, A. Kumamoto, S. Shirai, et al., "Electrostatic Electron Cyclotron Harmonic Waves Observed by the Akebono Satellite Near the Equatorial

- Region of the Plasmasphere,” *Earth, Planets and Space*, **59**, 6, June 2007, pp. 613–629.
4. J. Menietti, Y. Shprits, R. Horne, E. Woodfield, G. Hospodarsky, et al., “Chorus, ECH, and Z Mode Emissions Observed at Jupiter and Saturn and Possible Electron Acceleration,” *Journal of Geophysical Research: Space Physics*, **117**, A12, December 2012, p. A12214.
 5. M. Moncuquet, N. Meyer-Vernet, and S. Hoang, “Dispersion of Electrostatic Waves in the Lo Plasma Torus and Derived Electron Temperature,” *Journal of Geophysical Research: Space Physics*, **100**, A11, November 1995, pp. 21697-21708.
 6. R. Fredricks and F. Scarf, “Recent Studies of Magnetospheric Electric Field Emissions Above the Electron Gyrofrequency,” *Journal of Geophysical Research*, **78**, 1, January 1973, pp. 310-314.
 7. S. Kurita, Y. Miyoshi, C. M. Cully, V. Angelopoulos, O. L. Contel, et al., “Observational Evidence of Electron Pitch Angle Scattering Driven by ECH Waves,” *Geophysical Research Letters*, **41**, 22, October 2014, pp. 8076-8080.
 8. X. Zhang and V. Angelopoulos, “On the Relationship of Electrostatic Cyclotron Harmonic Emissions With Electron Injections and Dipolarization Fronts,” *Journal of Geophysical Research: Space Physics*, **119**, 4, March 2014, pp. 2536-2549.
 9. M. Fukizawa, T. Sakanoi, Y. Miyoshi, K. Hosokawa, K. Shiokawa, et al., “Electrostatic Electron Cyclotron Harmonic Waves as a Candidate to Cause Pulsating Auroras,” *Geophysical Research Letters*, **45**, 23, November 2018, pp. 12,661-12,668.
 10. Y. Miyoshi, I. Shinohara, T. Takashima, K. Asamura, N. Higashio, et al., “Geospace Exploration Project ERG,” *Earth, Planets and Space*, **70**, 1, June 2018, pp. 1-13.
 11. Y. Kasahara, Y. Kasaba, H. Kojima, S. Yagitani, K. Ishisaka, et al., “The Plasma Wave Experiment (PWE) on board the Arase (ERG) Satellite,” *Earth, Planets and Space*, **70**, 1, May 2018, pp. 1–28.
 12. S. Matsuda, Y. Kasahara, H. Kojima, Y. Kasaba, S. Yagitani, et al., “Onboard Software of Plasma Wave Experiment Aboard Arase: Instrument Management and Signal Processing of Waveform Capture/Onboard Frequency Analyzer,” *Earth, Planets and Space*, **70**, 1, May 2018, pp. 1-22.
 13. A. Matsuoka, M. Teramoto, R. Nomura, M. Nosé, A. Fujimoto, et al., “The ARASE (ERG) Magnetic Field Investigation,” *Earth, Planets and Space*, **70**, 1, March 2018, pp. 1-16.